# Superalkali-alkalide interactions and ion pairing in low-polarity solvents

René Riedel<sup>1\*</sup>, Andrew G. Seel<sup>2,3\*</sup>, Daniel Malko<sup>1</sup>, Daniel P. Miller<sup>4</sup>, Brendan T. Sperling<sup>4</sup>, Heungjae Choi<sup>5</sup>, Thomas Headen<sup>6</sup>, Eva Zurek<sup>7</sup>, Adrian Porch<sup>5</sup>, Anthony Kucernak<sup>1</sup>, Nicholas C. Pyper<sup>8</sup>, Peter P. Edwards<sup>2\*</sup>, Anthony G.M. Barrett<sup>1\*</sup>

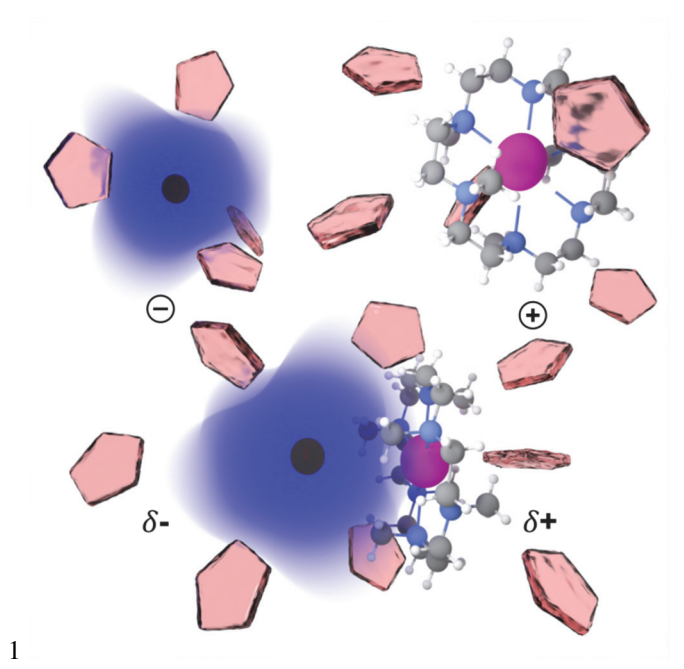
- <sup>1</sup> Department of Chemistry, Imperial College London, Molecular Sciences Research Hub, White City Campus, Wood Lane, London W<sub>12</sub> oBZ, UK.
- 2 Department of Physics and Astronomy, University College London, Gower Street, London WC1E 6BT, UK.
- 3 Inorganic Chemistry Laboratories, University of Oxford, Park Royal Road, Oxford OX1 3QR, UK.
- 4 Department of Chemistry, 106 Berliner Hall, Hofstra University, Hempstead, NY 11549, USA.
- 5 School of Engineering, Cardiff University, Cardiff CF24 3AA, UK.
- 6 ISIS Neutron and Muon Source, Science and Technology Facilities Council, Rutherford Appleton Laboratory, Harwell Campus, Didcot OX11 oQX, UK.
- 7 Department of Chemistry, 777 Natural Sciences Complex, State University of New York at Buffalo, Buffalo, NY 14260-3000, USA.
- 8 University Chemical Laboratory, Lensfield Road, Cambridge CB2 1EW, UK.

**ABSTRACT:** The nature of anionic alkali metals in solution is traditionally thought to be 'gas-like' and unperturbed. In contrast to this non-interacting picture, we herein present experimental and computational data that support ion pairing in alkalide solutions. Concentration dependent ionic conductivity, dielectric spectroscopy, and neutron scattering results are consistent with the presence of superalkali-alkalide ion pairs in solution, whose stability and properties have been further investigated by DFT calculations. Our temperature dependent alkali metal NMR measurements reveal that the dynamics of the alkalide species is both reversible and thermally activated, and suggest a complicated exchange process for the ion paired species. The results of this study go beyond a picture of alkalides being a 'gas-like' anion in solution, and highlight the significance of the interaction of the alkalide with its complex counter cation.

## 1 INTRODUCTION

- 2 Remarkably, anionic forms of the electropositive Group I
- 3 metals, with the exception of lithium, can be generated in
- 4 condensed phases.1 Termed alkalides, these monoanions
- 5 are chemically highly reducing and possess a diffuse,
- 6 closed-shell ns<sup>2</sup> configuration, resulting in an exceptional-
- 7 ly high electronic polarizability. The formation and stabi-
- 7 ly high electronic polarizability. The formation and stabi-
- 8 lization of alkalide species requires stringent chemical
- 9 environments and involves either a disproportionation or
- 10 the reduction of one elemental alkali metal by another.2
- 11 The dissolution and reduction process is facilitated by
- 12 recuision and reduction process is facilitated by
- 12 strong stabilization of the alkali cation by pre-organized
- 13 complexants such as crown ethers and cryptands.3 This
- 14 enables alkali metals to be dissolved in even weakly polar
- 15 solvents such as tetrahydrofuran (THF) by formation of
- 16 alkalide anions that persist in the absence of any better 17 electron receptor, such as ammonia or small amines
- 18 (metal-ammonia solutions<sup>4-6</sup> and formation of solvated
- 19 electrons<sup>7,8</sup>), functional groups in organic or organometal-
- 20 lic molecules (the Dissolving Metal Reduction), or simply

- 21 a different more reducible metal. Cryogenic temperatures 22 are also necessitated in solution to avoid reduction and
- 23 decomposition of solvent.



2 **Figure 1.** Illustration of potential components of a sodide 3 solution in HMHC/THF. Separately solvated complexed po-4 tassium (pink) cation (top left) and alkalide anion (top right) 5 with its diffuse 3s<sup>2</sup> valence orbital (blue) and a contact ion 6 pair (bottom) in a medium of THF molecules (red) are indi-7 cated.

8 Perhaps the most puzzling aspect of alkalides, which has 9 persisted almost from the time of their discovery, is an 10 understanding of the precise nature of their diffuse ns<sup>2</sup> 11 orbital in solution. The NMR signatures of an alkalide 12 species in solution, and in the crystalline solids they form, 13 are significantly shielded and exhibit an exceptionally 14 narrow line width. Considering that the alkali metals all 15 possess quadrupolar nuclei, these features have been as-16 cribed to the high shielding and high symmetry of an un-17 perturbed 'gas-like' anion in solution, with little to no 18 interaction with its local environment.9-14 However, the 19 high polarizability of the alkalides and ready electron dis-20 sociation into solvated-electron species with increasing 21 solvent polarity imply that the genuine alkalide could be 22 significantly perturbed in solution in certain cases. In-23 deed, the 'gas-like' picture of alkalides in solution has 24 recently been questioned by ab initio calculations, which 25 have instead provided two insights in favor of a picture of 26 an alkalide interacting with its environment: Firstly, it 27 was suggested that the most stable species were formed 28 via the association of the alkalide anion with solvat-29 ed/complexed alkali cations in a known alkalide-forming 30 solvent, 1,2-ethylenediamine,15 and it was shown that the 31 simulated absorption spectra for such interacting species 32 in the visible and ultraviolet ranges were in agreement 33 with experimental observations. The complexed alkali 34 metal cations have been termed 'superalkali' cations be-35 cause their LUMOs are highly expanded but retain similar 36 symmetries to those of the uncomplexed alkali metal cat-37 ions, and able to accept electron density from the alkalide 38 in a weak donor-acceptor sense. Secondly, molecular dy-39 namics simulations on explicitly solvated sodide (Na<sup>-</sup>)

40 ions suggested that the expanded 3s<sup>2</sup> orbital is perturbed 41 by its environment, but the NMR response for the sodium 42 nucleus is negligibly affected, despite its quadrupolar na-43 ture.<sup>16</sup>

44 Here we provide experimental evidence that alkalides 45 interact with their environment through the formation of 46 ion paired species in solution (see Figure 1). Further sup-47 port is provided by Density Functional Theory (DFT) cal-48 culations that suggest a nature beyond that of classic ion 49 associates.<sup>17</sup> Such weakly covalent interactions between 50 the alkalide and the counter superalkali cation reflect a 51 subtle chemistry for alkalides, which has previously not 52 been reported. As such, our findings have implications for 53 future control of alkalide properties, and their potential 54 use in photo- and electrochemical applications.

# 55

#### **56 EXPERIMENTAL SECTION**

57 Full experimental details and characterization regarding 58 the preparation of HMHC are provided in the Supporting 59 Information. Crude HMHC and commercially available 60 15-crown-5 were purified by Kugelrohr distillation from 61 NaK, kept under an argon atmosphere and handled inside 62 an argon glovebox.

63 Ionic conductivity measurements. Impedance meas-64 urements were carried out using a potentiostat Gamry 65 Reference 600 and using platinized platinum electrodes 66 (cell constant 0.98 cm). The Walden product was calcu-67 lated using the shear viscosity of metal-free solutions of 68 15-crown-5 in THF at all relevant concentrations as an 69 approximation of the viscosity of metal solutions. The 70 shear viscosity was determined over the temperature 71 range of 15–40 °C using a RheoSense m-VROC viscometer. 72 In a typical experiment, NaK was added in small portions 73 (< 20 mg) to a solution of 0.06 M 15-crown-5 or 0.03 M 74 HMHC in dry THF at 243 K while the conductivity of the 75 mixture was monitored in set intervals of 0.5 min. Macro-76 cycle concentration was doubled when the concentration 77 of dissolved metal reached approximately 70% saturation 78 to maintain a sufficient metal dissolution rate. The ratio 79 between metal and macrocycle concentration at a given 80 metal concentration was found to have no effect on the 81 conductivity.

82 **Small angle neutron scattering (SANS).** SANS spectra 83 were collected at the neutron diffractometer NIMROD<sup>18</sup> 84 at the ISIS Neutron and Muon Source Facility, UK. Sam-85 ples were prepared by mixing of all components (HMHC 86 (1 equiv.) or 15-crown-5 (2 equiv.), d<sub>8</sub>-THF, NaK (n/n 1:1, 87 3 equiv.)) in a quartz NMR tube inside an argon glovebox 88 with a cryogenic and inert atmosphere being maintained. 89 Samples were then warmed to 240 K and equilibration for 90 10 h prior to measurement ensured complete metal disso-91 lution up to a point of saturation. Data were reduced us-92 ing standardized procedures within the GudrunN soft-93 ware. Density values were precisely determined for all 94 relevant metal-free complexant solutions in protiated 95 THF using a 4 place digital *LiquiPhysics* Excellence den-96 sity meter DM40 over the temperature range of 273-303 K.

1 Density values at 243 K were determined by linear extrap-2 olation (Details provided in the Supporting Information).

3 **Density functional theory details.** The DFT calcula-4 tions performed used the Perdew-Burke-Ernzerhof (PBE) 5 functional<sup>20</sup> with the Amsterdam Density Functional 6 (ADF)<sup>21-23</sup> software package. TZP basis sets from the ADF 7 basis set library were used for the Na, K, C, N, and O at-8 oms, while the QZ<sub>3</sub>P + 1 diffuse function basis set was 9 used for the H atoms.<sup>24</sup> The core electronic states were 10 kept frozen for all atoms except Na and K. Further com-11 putational details are provided in the Supporting Infor-12 mation, Section S<sub>7</sub>.

13 NMR spectroscopy. <sup>23</sup>Na NMR spectra were acquired at 14 106 MHz on a Bruker DRX-400 spectrometer. 39K NMR 15 spectra were acquired at 28 MHz on a Bruker Avance 16 600 MHz NMR spectrometer. Chemical shifts are report-17 ed as  $\delta$ -values in ppm relative to the cation signal from 18 external aqueous solutions of the respective chloride salt 19 at room temperature. Samples were prepared by addition 20 of all components (complexant HMHC (1 equiv.) or 15-21 crown-5 (2 equiv.), d<sub>8</sub>-THF, NaK (3 equiv.)) to an oven-22 and flame-dried borosilicate NMR tube with J Young 23 valve inside an argon glovebox. The sealed tubes were 24 removed from the glovebox and cooled to 195 K before 25 exposure of the metal alloy to the solution. The samples 26 were stored at 195 K and warmed to 240 K for 10 h in 27 preparation for the respective NMR experiment to ensure 28 complete metal dissolution up to a point of saturation. 29 The probe of the NMR spectrometer was cooled to 200 K 30 prior to quick sample loading. The steady reduction in 31 signal intensity upon thermal cycling is reversible, whilst 32 taking into account a slight loss of intensity over time due 33 to minor decomposition processes. All measurements 34 were corrected for any loss in signal intensity due to a 35 shift of the Boltzmann distribution of spin states.

#### 37 RESULTS AND DISCUSSION

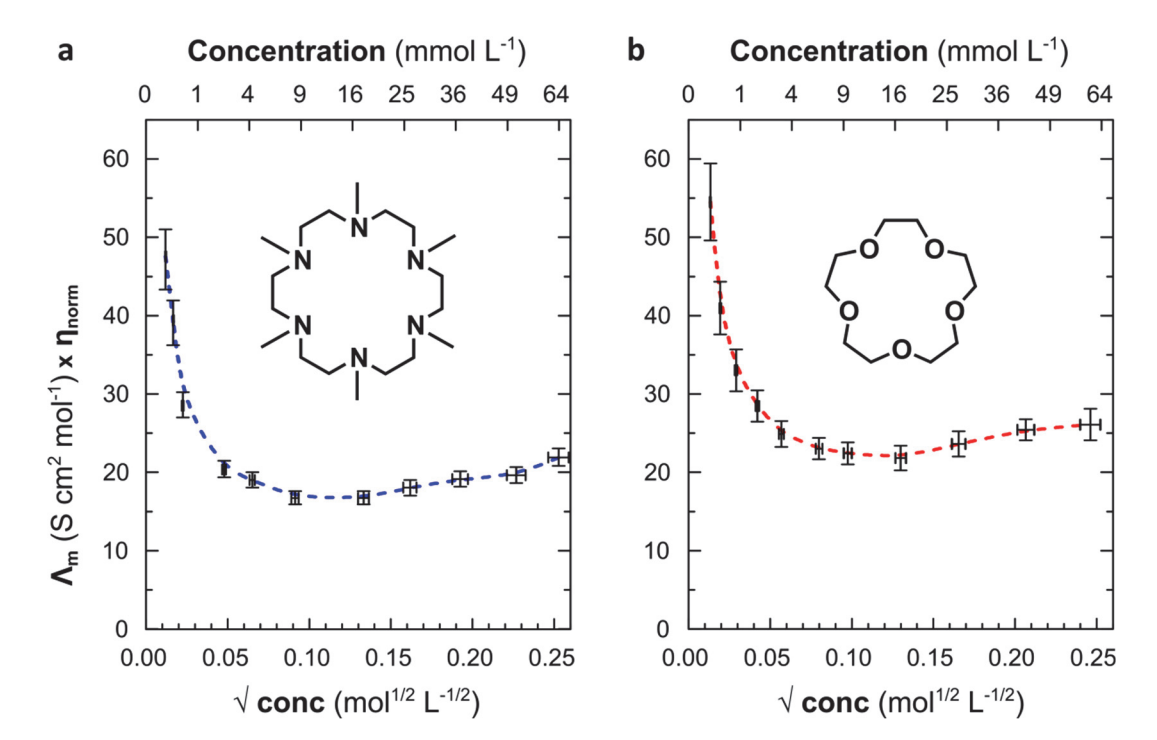
38 Design and control of chemical composition. The 39 accurate preparation and investigation of alkalide solu-40 tions, especially at concentrations as low as those shown 41 in Figure 2, requires the use of complexing agents that 42 are resistant to irreversible reductive ring scission. A 43 milestone in the development of more stable alkalide sys-44 tems was the introduction of per-alkylated polyamine 45 ligands to the field.25 This showed that the hexa-aza-1,4,7,10,13,16-hexamethyl-1,4,7,10,13,16-hexaaza-46 crown 47 cyclooctadecane (hexamethyl-hexacyclen, HMHC, see 48 Error! Reference source not found.) significantly out-49 performs the reportedly most stable crown ether 15-50 crown-5<sup>26</sup> in its resistance to reductive decomposition in 51 the presence of alkalides. THF was found to be the most 52 suitable organic solvent as it allowed for a comparably 53 rapid metal dissolution, and for the preparation of alka-54 lide solutions with exceptionally high metal concentra-55 tions and long-lived stability and persistence. Error! Ref-56 erence source not found. highlights the stark contrast 57 in stability between the metal solutions using HMHC and 58 the more labile complexant 15-crown-5 in THF, which was

59 ascribed to the decreased reactivity of C–N bonds as com-60 pared to C-O bonds under strongly reducing conditions.

a Conductivity [µS/cm] b Stability at RT VS. 15C5 vs. HMHC Concentration [ppm] 2.0 | 0.5 24 h 3.2 | 0.9 48 h 4.0 | 1.2 5.5 | 1.9 **HMHC** 

63 **Figure 2.** Alkalide solutions in low-polarity solvent tetrahy-64 drofuran (THF). (a) Relation between concentration, con-65 ductivity, and color intensity of characteristically blue sodide 66 solutions in 50 mL THF at extremely high dilution. (b) Sta-67 bility of solutions of NaK in 40 mM 15-crown-5/THF (left) 68 and 20 mM HMHC/THF (right) in the presence of NaK after 69 storage at room temperature for 24 h (top) and 48 h (bot-70 tom) and structural formulae of aza-crown HMHC and 71 crown ether 15-crown-5 (15C5) used in this work.

15C5



2 **Figure 3.** Walden product vs. square-root of the concentration of sodide solutions. (a) Concentration dependent Walden prod-3 uct of solutions of NaK in 15-crown-5 in THF at 243 K. (b) Concentration dependent Walden product of solutions of NaK in 4 HMHC in THF at 243 K. Dashed lines represent guides to the eye.

6 Ionic Conductivity and Small Angle Neutron Scatter-7 ing (SANS). Investigation of the concentration depend-8 ence of ionic conductivity of electrolyte solutions is the 9 acknowledged technique to interrogate the nature of ion 10 association in solution. Our experimental methodology 11 allowed for the reproducible preparation of highly dilute 12 metal solutions (Figure 2) and the accurate determina-13 tion of their metal content by ion chromatography, ena-14 bling the investigation of conductivity across a wide con-15 centration range. Plots of the relationship between con-16 centration and the associated Walden product for solu-17 tions of NaK in 15-crown-5/THF and HMHC/THF 18 (Figure 3) show that both exhibit a rapid decrease fol-19 lowed by a slight increase of the derived Walden product 20 with increasing metal concentration. While the decrease 21 in molar conductivity is a familiar consequence of ion 22 association, the presence of a minimum at ~15 mM distin-23 guishes the Walden product trend of the alkalide systems 24 from that of a classic weak electrolyte. Such conductance 25 minima have been reported for several solutions of elec-26 trolytes and ionic liquids in low-polarity solvents<sup>27-37</sup> and 27 agree with the theory of a feedback between the ion asso-28 ciation equilibrium and the overall relative permittivity of 29 mixtures in low-polarity solvents.31,38-42 Examination of the 30 frequency-dependent dielectric spectra and monitoring of 31 the static permittivity over the period of metal dissolution 32 yields results that are consistent with an increase of the 33 overall relative permittivity of the solution due to an in-34 creasing number of ion pairs upon metal dissolution 35 (Supporting Information, Figure SI-4).

1

5

36 We employed neutron scattering measurements to exam-37 ine any structural signatures for such associations. The 38 length scales of the macrocycle-encapsulated cation or 39 the envisaged contact- ion / ion paired superalkali-40 alkalide correspond to a range in reciprocal space that is 41 intermediary between that probed in small and wide-42 angle neutron scattering, with intramolecular distances 43 overlapping with intermolecular, solvent-solvent or sol-44 vent-solute distances. The use of a protiated macrocycle 45 and deuterated solvent overcomes this problem due to 46 the large difference in coherent neutron scattering length 47 of the proton (-3.74 fm) and the deuteron (6.67 fm). This 48 enables the macrocyclic complex to behave as a scattering 49 object in the limit of low scattering angle Q, and any 50 change to its size/solvation via the association of the alka-51 lide should be apparent. Within the low-Q limit, the co-52 herent differential neutron scattering cross section,  $\frac{d\sigma}{d\theta}$ , is 53 given by

$$54 \frac{\mathrm{d}\sigma}{\mathrm{d}\rho} = N V_P^2 (\Delta \rho)^2 P(Q), \qquad (1)$$

55 where N is the number of scattering objects of volume  $V_P$ , 56  $\Delta \rho$  is the contrast between the scattering-length density 57 of the object and the average scattering-length density of 58 the solvent, and P(Q) is the form- or shape-factor for the 59 object. This expression holds only for the dilute limit, 60 where there are no significant "object-object" correlations 61 in the solution.

Table 1. Molecular parameters from DFT models of superalkalis and superalkali-alkalide pairs.<sup>a</sup>

	Binding Energy <sup>b</sup> (kJ/mol)	MM Distance (Å)	Superalkali Hirshfeld Charge (e)	Alkalide Hirshfeld Charge (e)	Dipole Moment / (D)
Superalkali M-15-crown-5₂ Mode	ls				
Na-15-crown-52	-84.5	-	+0.26	-	4.5
K-15-crown-52	-109.7	-	+0.23	-	2.7
Superalkali-Alkalide Pair M-15-crown-52 (M) Models					
Na-15-crown-52 (Na)	-147.4	5.71	+0.28	-0.45	17.1
K-15-crown-5₂ (Na) – Equatorial	-178.2	5.59	+0.28	-0.42	15.6
K-15-crown-5₂ (Na) – Axial	-177.7	6.20	+0.27	-0.43	18.3
Na-15-crown-52 (K)	-132.9	6.38	+0.28	-0.42	17.0
K-15-crown-5₂ (K)	-166.7	7.08	+0.28	-0.43	17.9
Superalkali M-HMHC Models					
Na-HMHC	-62.7	-	+0.31	-	o
K-HMHC	-90.9	-	+0.26	-	О
Superalkali-Alkalide Pair M-HM	HC (M) Models				
Na-HMHC (Na)	-152.0	3.61	+0.22	-0.23	9.3
K-HMHC (Na) – Chair <sup>c,d</sup>	-177.0	4.11	+0.24	-0.29	10.6
K-HMHC (Na) – Boat <sup>c,d</sup>	-183.5 (-150.6)	4.00 (4.50)	+0.21 (+0.27)	-0.29 (-0.33)	10.5 (12.6)
Na-HMHC (K)	-130.8	4.36	+0.25	-0.21	9.8
K-HMHC (K)	-159.0	4.73	+0.25	-0.24	9.9

<sup>&</sup>lt;sup>a</sup> M is the symbol for the alkali metal, to represent either Na or K. Each HMHC system given was modelled with the chair conformation, except for the 'K-HMHC (Na) – Boat' where the most stable and least stable positions of the sodide are given outside and within the parentheses, respectively. Each 15-crown-52 system was modelled as the equatorial pair unless labelled differently. M-HMHC and M-15-crown-52 are referred to as superalkalis.

Figure 3 presents neutron scattering data for both alkalide solutions (15-crown-5 or HMHC in THF with and without dissolved K<sup>+</sup> Na<sup>-</sup>) and control solutions of either 15-crown-5 or HMHC in D<sub>2</sub>O both with and without dissolved K<sup>+</sup> I<sup>-</sup>. These control solutions were chosen to represent fully ion-dissociated systems of separately solvated macrocycle-K<sup>+</sup> and I<sup>-</sup>.

Furthermore, the iodide and sodide anions are almost identical in size and possess similar coherent neutron scattering lengths. It is apparent from Figure 4 that the alkalide solutions both possess an increase in small-angle intensity whereas the control systems containing iodide do not exhibit such an increase. Importantly, this indicates that the scattering behavior of the macrocycle complex does not change in the control (as expected from simply binding K<sup>+</sup> with its extremely low neutron scattering length and negligible contribution to scattering from the macrocycle complex), whereas in the alkalide systems the scattering volume and contrast has clearly increased.

Simple ellipsoidal form factor models are reported in the Supporting Information in Figure SI-5 and are concordant with an association of the alkalide with the macrocyclic superalkali, effectively increasing the effective volume of scattering object in solution from that of a solvated macrocycle to a solvated superalkali-alkalide ion pair. Moreover, a larger aggregation of ions in solution would lead to a small angle signal orders of magnitude higher than those witnessed in the alkalide solutions, thus enabling us to rule out any macroscopic phase separation or higher alkalide agglomerates in the solutions.

<sup>&</sup>lt;sup>b</sup> The binding energies (BE in kJ/mol), calculated in the gas-phase by subtracting the energy of the alkali metal(s) and 15-crown-5/HMHC from the total system energy (see the Supporting Information, Equations S1, S2, S4 and S5).

<sup>&</sup>lt;sup>c</sup> The BEs were calculated using the HMHC conformation adopted in the M-HMHC(M) model.

 $<sup>^{</sup>d}$  E[K-HMHC (Na) - chair] - E[K-HMHC (Na) - boat] = 0.84 kJ/mol.

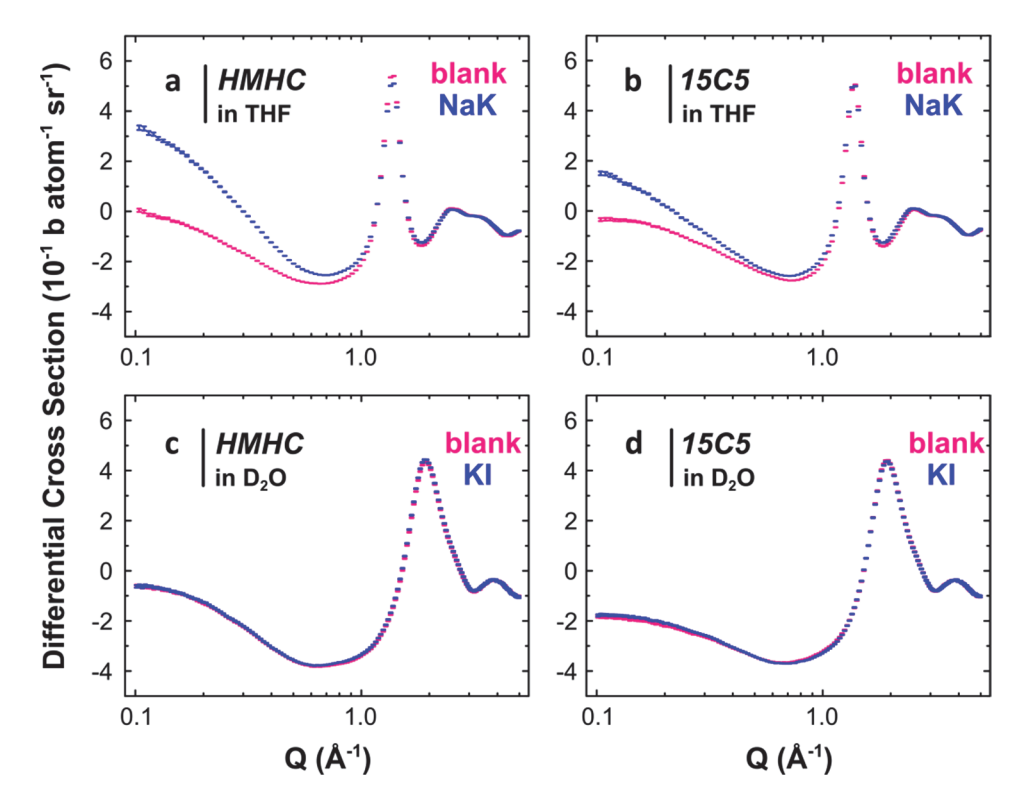


**Figure 4.** Small angle neutron scattering spectra for macrocycle solutions of both NaK in THF and KI in  $D_2O$ . Coherent differential cross section of blank (pink) and ion-containing (blue) solutions involving HMHC in THF- $d_8$  (0.05 M, **a**) and  $D_2O$  (0.05 M, **c**) and 15-crown-5 in THF- $d_8$  (0.1 M, **b**), and 15-crown-5 in  $D_2O$  (0.1 M, **d**).

**Ab** initio Calculations. To assess the possible species that may form in alkalide solutions, DFT calculations were performed on sodium and potassium superalkalis of HMHC and 15-crown-5, superalkali-alkalide ion pairs, and superalkali dimers. As shown in Table 1, K was calculated to interact more strongly than Na with both HMHC and 15-crown-5. The computed binding energies (BEs) suggest that the metal atoms prefer to be coordinated to two 15crown-5 molecules as opposed to a single complexant (Supporting Information, Section S15). In agreement with prior DFT calculations,15 the superalkali dimers were found to be less stable than the superalkali-alkalide ion pairs when solvation effects were considered (Supporting Information Section S14). Therefore, in this discussion we focus on the superalkali-alkalide ion pairs whose computed BEs and selected properties are given in Table 1, with optimized geometries and molecular orbitals illustrated in Figures 4 and 5. Out of the four metal combinations that are possible the encapsulated potassium and anionic sodide models, K-HMHC (Na) and K-15-crown-52 (Na), each possess the largest BEs, in agreement with the experimental observation of a predominance of potassium cations and sodide anions.

The flexibility of the macrocycles and approach of the second metal ion allows for several conformationally and topologically different superalkali-alkalide contact ion pairs. In its complexes with alkali cations, HMHC can adopt a conformation with all six nitrogen atoms in a single plane, similar to the chair conformation in the crystal-

line salt of K-HMHC with tetraphenylborate, 43 or by adopting a boat conformation, as is the case for the crystalline sodide K-HMHC (Na)44,45 (Figure 5). For the 15crown-5 systems, an alkalide can approach either axial or equatorial to the superalkali complex (Figure 6). These two systems are essentially isoenergetic, although the equatorial approach is statistically preferred. The chair and boat forms of K-HMHC (Na) are also isoenergetic, but pure HMHC favors the chair conformation by 5.9 kJ/mol. Calculations exploring the potential energy landscape associated with flipping the HMHC between the chair and boat conformations, both for pure HMHC and within the superalkali-alkalide complex, concluded that the chair form is the dominant species in solution (Supporting Information Section S16). Therefore, we focus upon the chair HMHC in this discussion.

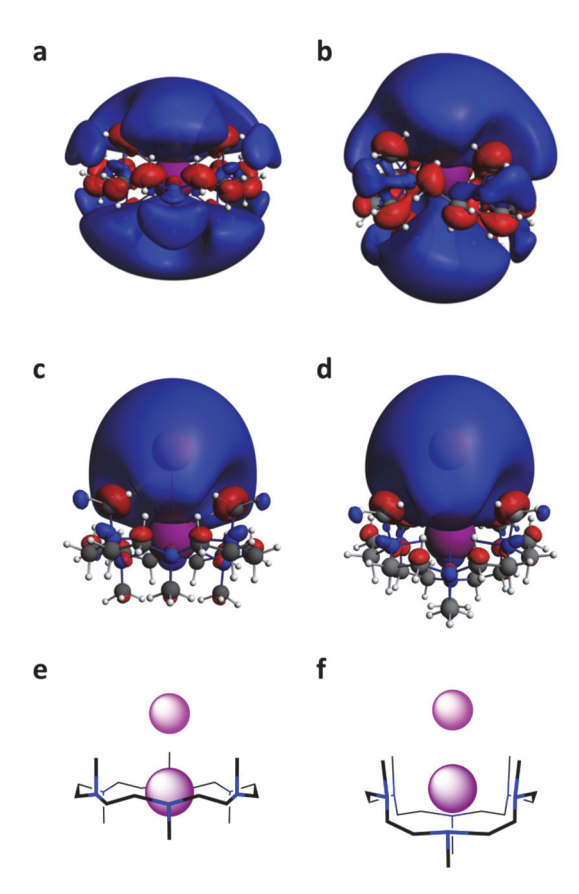


**Figure 5.** Computed SOMOs/HOMOs of superalkali K-HMHC and superalkali-alkalide K-HMHC<sup> $\delta$ +</sup>(Na) $^{\delta}$ -. Isosurfaces (Isovalue = +/- 0.010 a.u.) for superalkali models K-HMHC in the chair (a) and boat (b) conformations, and for the superalkali-alkalide models K-HMHC (Na) in the chair (c) and boat (d) conformations (Ion pairs in the chair (e) and boat (f) conformations illustrated in the form of a cartoon).

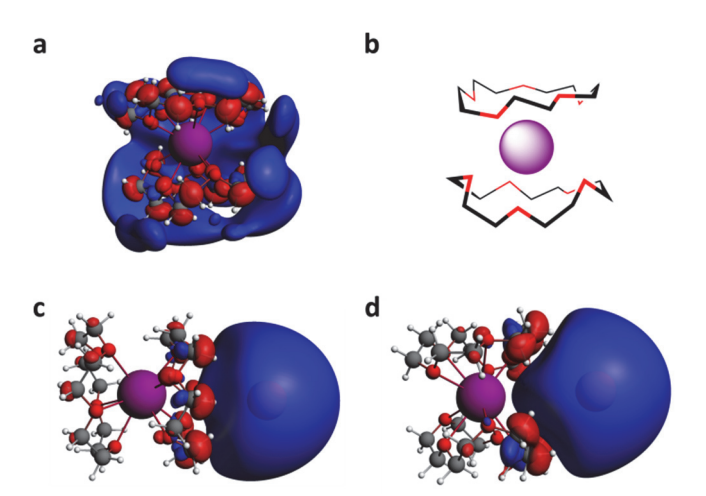


**Figure 6.** Computed SOMO/HOMOs of superalkali K-15-crown-52 and superalkali-alkalide K-15-crown- $5_2^{\delta+}$ (Na) $^{\delta-}$ . Isosurfaces (Isovalue = +/- 0.010 a.u.) for superalkali model K-15-crown- $5_2$  (**a**) and superalkali-alkalide K-15-crown- $5_2$  (Na) with the alkalide in the axial (**c**) and equatorial (**d**) positions with respect to the sandwich complex (as illustrated in the form of a cartoon (**b**)).

Turning to the NMR parameters, the computed shielding constant for the sodide in K-HMHC (Na) is 40-46 ppm larger than for the sodium cation in Na-HMHC (K) / Na-HMHC (Na). The Hirshfeld charges capture the loss of electron density from the encapsulated metal atom and an increase in electron density on the surrounding metal for all ion paired systems, as expected for the alkalide state being maintained even in a close ion pair. Both K-HMHC (Na) and K-15-crown-52 (Na) possess significant dipole moments, in line with the rationale behind the experimentally observed increase in molar conductivity at higher alkalide concentrations (Figure 3), and further ruling out weakly dipolar superalkali dimers (Supporting Information Table SI-4).

The HMHC superalkali C<sub>i</sub> symmetry SOMO extends from the metal symmetrically surrounding the superalkali above and below, in contrast to the 15-crown-52 superalkali C<sub>1</sub> symmetry SOMO that persists about the ether rings but does not have much character near the alkali metal (c.f. Figures 4 and 5). The HOMOs of the superalkali-alkalide complexes are concentrated on the sodide component, and they have a large spatial extent past the alkalide portion of the ion pair, in agreement with our neutron scattering results, and with the crystallographically derived radii of alkalides in the solid state. These HOMOs are formed from a bonding in-phase interaction between the SOMO of the sodium atom with the SOMO of the potassium superalkali, which itself contains character from the LUMOs of the complexant, as well as 4s and 5s K orbitals. The bond orders of 0.65 and 0.57 computed between K and Na highlight the partial covalency of the interaction in K-HMHC (Na) and K-15-crown-52 (Na), respectively. Additional stability in these superalkali and superalkali-alkalide complexes, alongside coordination and Mô+Mô- pairing, originates from intramolecular H H interactions first introduced in Ref. [5] to denote the bonding between hydrogen atoms due to orbital overlap in a crucial occupied bonding orbital. In the superalkali and superalkali-alkalide complexes this interaction is evident in the SOMOs and HOMOs (Figures 4, 5, and Supporting Information Figures SI-9-14, SI-21). This H \*\*\* H bonding arises from the partial population of the LUMO of the organic species when alkali metals are introduced to the system (Supporting Information Figures that the distance between pairs of hydrogen atoms is ~0.1 Å shorter in the superalkali systems as compared to pure HMHC and 15-crown-5.

Variable temperature NMR spectroscopy. <sup>23</sup>Na and <sup>39</sup>K NMR spectra under cryogenic conditions exhibit the expected narrow, shielded signals in concentrated solutions of macrocycle/NaK and macrocycle/K in THF, respectively (Figure 7 and Supporting Information Figure SI-1). The dynamics of the alkalide species, their interactions with their local environment or with other components in solution, are evidenced through comparison of <sup>23</sup>Na spectra at different temperatures over an accessible range of more than 60 K (Figure 7). Increasing the temperature results in a rapid and reversible decrease in the total integrated

area of signals in the chemical shift range of (-61) – (-63) ppm for both macrocycle systems.

Considering the lack of any additional signals in the chemical shift range of (+100) – (-200) ppm, we attribute the unusual behavior of alkalide species in NMR to an exchange process between an NMR-visible and an NMR-invisible species, each involving the alkali metal nucleus of interest. The line width of the alkalide signal increases only slightly from 2.9 Hz to 9.0 Hz from 235 to 290 K despite the drastic loss in signal intensity. This suggests a thermally activated transformation of the NMR-visible species in the slow exchange limit.<sup>46</sup> Very minor changes in the chemical shift of the signals cannot be conclusively demonstrated here due to the sensitive temperature dependence of the reference signal.

If the relaxation of the quadrupolar alkalide nucleus were purely due to the approach of the superalkali counter cation, it must be induced by a sufficiently large electric field gradient (EFG) at the alkalide nucleus. However, our computed EFG, Vzz, does not differ from the isolated sodide to the ion pair and is essentially o relative to the computed Vzz for Na and K in the superalkali (Supporting Information Tables SI-5, SI-7). Recent results from ab initio molecular dynamics showed that the sodide anion may appear in NMR experiments as if it were an unperturbed, spherical ion, despite the polarizable 3s orbital being strongly affected by the surrounding species in solution.<sup>16</sup> We note that the solvent modeled in Ref. 16 was methylamine, a solvent of higher dielectric than the THF solutions used in this study, and which would be expected to perturb the alkalide species to an even greater extent. Hence, we conclude that the NMR-visible alkalide species is subject to a fast and reversible exchange process with an NMR invisible species, which is particularly short lived. This may be a paramagnetic species or a chargetransfer state but is not due to the association and dissociation of the superalkali-alkalide complex.

Another interesting and exclusive feature of the HMHC sodide system observed upon close inspection of the <sup>23</sup>Na NMR is the existence of a small shoulder in the major signal on the low-field side (Figure 7a). This shoulder becomes more pronounced as the signals drift apart with decreasing temperature. The small difference in chemical shift between the primary and secondary signals around the -60 ppm chemical shift range suggests the involvement of a coordinative or, more likely, a conformational difference between both NMR-visible species without a loss of its integrity.

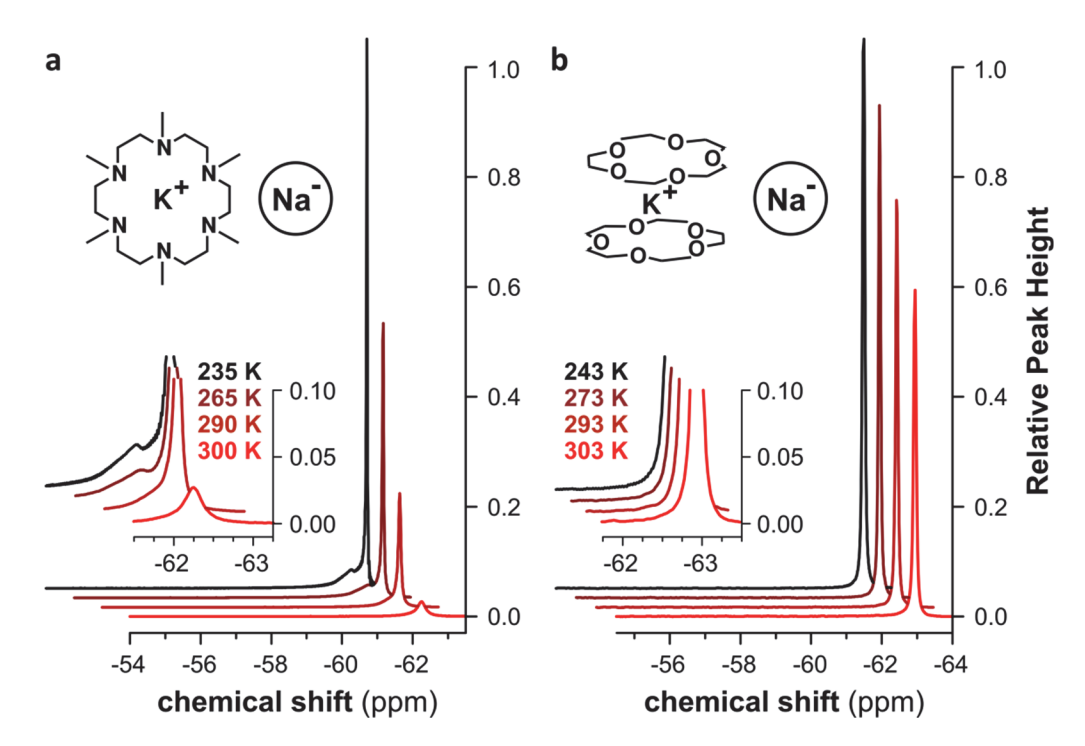


**Figure 7.** Temperature dependent <sup>23</sup>Na NMR spectroscopy of sodide solutions in THF. (a) Upfield range of <sup>23</sup>Na spectra showing the temperature dependent change in shape and total signal intensity of the alkalide signal of a solution of 0.3 M NaK in HMHC/THF in the chemical shift range between (-61) – (-65) ppm. (b) Upfield range of <sup>23</sup>Na spectra showing the temperature dependent change in shape and total signal intensity of the alkalide signal of a solution of 0.4 M NaK in 15-crown-5/THF in the chemical shift range between (-61) – (-65) ppm. Spectra are referenced to 1 M aq. NaCl solution at room temperature according to IUPAC recommendations and normalized to the intensity at the lowest recorded temperature, respectively. Insets show zooms of the signal onsets.

Mindful of our above discussion concerning the effect of a perturbation of the alkalide on its NMR signature, we suggest that this is due to the conformational flexibility of the superalkali-alkalide complex of HMHC that is absent in the 15-crown-5 case, bearing in mind that both chair like and boat like conformations for the HMHC macrocycle exist in crystalline systems. Clearly, much further work remains as to identifying the precise nature, and mechanisms, of these intriguing exchange processes

#### CONCLUSION

Alkalides have a unique place in the history and chemistry of the s-block elements.¹ Since their discovery by J. L. Dye and colleagues the characterization of the alkalide species in condensed matter systems has led to the fascinating discussion of their diffuse, yet localized, electronic states in weakly polar solvents, and indeed to the application of alkalides as highly reductive species across chemistry.²5-47-49 The existence of ion paired species has been mooted since the very earliest discussions of alkalides, but has never been experimentally demonstrated conclusively.

Herein, we have provided experimental evidence of the observation and effect of ion pairing of alkalides in solution, both from examination of their macroscopic conductivity and dielectric properties, to the local disruption of

solvent scattering density witnessed in coherent neutron scattering. To suggest what form these ion pairs may take in solution, we have carried out DFT calculations on a number of possible superalkali-alkalide complexes in addition to superalkalis and superalkali dimers. In agreement with recent ab initio results, 16 our models implicate that the superalkali-alkalide complex, which we suggest is the dominant species in solution, may be indistinguishable in NMR from an isolated solvated alkalide and so we have revisited the classical interpretation of such data in the literature of alkalides. We attach great importance to the temperature dependence of the conformationally dynamic HMHC system, indicating that there is much more to be understood as to the kinetics of alkalides in solution: The reversible perturbation and possible disintegration of the NMR-visible species (that may well be the contact ion-pair) highlights the significance of the interaction of alkalides with their complex counter-cations.

Our studies paint a picture of an alkalide species being far beyond a 'gas-like' ion in solution, but instead one that could be 'chemically' controlled and developed by considering superalkali-alkalide interactions of the sort delineated here. We believe that the interactions of alkalides in solution is merely the most recent in a long line of surprising and unique aspects of s-block chemistry, and certainly one that has the potential to affect how these systems are extended and applied in the future.

#### ASSOCIATED CONTENT

**Supporting Information**. Experimental protocols and full characterization, NMR data, description of ionic conductivity methodology, dielectric spectroscopy methodology and data, computational details, isosurfaces illustrations, structure coordinates. This material is available free of charge via the Internet at http://pubs.acs.org.

#### **AUTHOR INFORMATION**

### **Corresponding Authors**

rene.riedel13@imperial.ac.uk a.seel@ucl.ac.uk peter.edwards@chem.ox.ac.uk agm.barrett@imperial.ac.uk

#### **ACKNOWLEDGMENT**

We thank GSK for support to A.G.M.B. with the Glaxo endowment. This work is part-funded by the European Regional Development Fund through the Welsh Government. Experiments at the ISIS Neutron and Muon Source were supported by a beamtime allocation RB1810754 from the Science and Technology Facilities Council. D.P.M. and E.Z. thank the Center for Computational Research at the University at Buffalo, SUNY for computational support.<sup>50</sup> D.P.M. thanks Hofstra University for funding through a Faculty Research and Development Grant (FRDG). E.Z. acknowledges the NSF (DMR-1827815) for financial support, and Jochen Autschbach for valuable discussions.

#### **ABBREVIATIONS**

15C5, 15-crown-5; DFT, density functional theory; EFG, electric field gradient; HMHC, 1,4,7,10,13,16-hexamethyl-1,4,7,10,13,16-hexaazacyclooctadecane; HOMO, highest occupied molecular orbital; LUMO, lowest unoccupied molecular orbital; NMR, nuclear magnetic resonance; SANS, small angle neutron scattering; SOMO, singly occupied molecular orbital; THF, tetrahydrofuran.

## **REFERENCES**

- (1) Dye, J. L. The alkali metals: 200 years of surprises. *Phil. Trans. R. Soc. A* **2015**, 373, 174–187.
- (2) Dye, J. L. Compounds of alkali metal anions. *Angew. Chem. Int. Ed.* **2009**, *18*, 587-598.
- (3) Dye, J. L.; Redko, M. Y.; Huang, R. H.; Jackson, J. E. Role of cation complexants in the synthesis of alkalides and electrides. *Adv. Inorg. Chem.* **2006**, *59*, 205-231.
- (4) Thompson, J. C. *Electrons in Liquid Ammonia* (Oxford Univ. Press, Oxford, 1976).
- (5) Zurek, E.; Edwards, P. P.; Hoffmann, R. A molecular perspective on lithium-ammonia solutions. *Angew. Chem. Int. Ed.* **2009**, *48*, 8198-8232.
- (6) Catterall, R.; Mott, N. F. Metal-ammonia solutions. *Advances in Physics* **1969**, *18*, 665-680.
- (7) Buttersack, T.; Masoni, Ph. E.; McMullen, R. S.; Schewe, H. Ch.; Martinek, T.; Brezina, K.; Crhan, M.; Gomez, A.; Hein, D.; Wartner, G.; Seidel, R.; Ali, H.; Thürmer, S.; Marsalek, O.; Winter, B.; Bradforth, S. E.; Jungwirth, P. Photoelectron spectra of alkali metal-ammonia microjets: From blue electrolyte to bronze metal. *Science* **2020**, *368*, 1086-1091.
- (8) Hartweg, S.; West, A. H. C.; Yoder, B. L.; Signorell, R. Metal transition in sodium–ammonia nanodroplets. *Angew. Chem. Int. Ed.* **2016**, 55, 12347-12350.

- (9) Ceraso, J. M.; Dye, J. L. <sup>23</sup>Na NMR spectrum of the sodium anion. *J. Chem. Phys.* **1974**, *61*, 1585.
- (10) Edwards, P. P.; Ellaboudy, A. S.; Holton, D. M. NMR spectrum of the potassium anion K. *Nature* **1985**, *317*, 242-244.
- (11) Tinkham, M. L.; Dye, J. L. First observation by potassium-39 NMR of K<sup>-</sup> in solution and in crystalline potassides. *J. Am. Chem. Soc.* **1985**, *107*, 6129-6130.
- (12) Ellaboudy, A. S.; Holton, D. M.; Pyper, N. C.; Edwards, P. P.; Wood, B.; McFarlane, W. Gas like nature of the sodium anion in solution. *Nature* 1986, 321, 684-685.
- (13) Holton, D. M.; Ellaboudy, A.; Pyper, N. C.; Edwards, P.P. Nuclear spin-lattice relaxation in the sodium anion, Na<sup>-</sup>. *J. Chem. Phys.* **1986**, *84*, 1089.
- (14) Pyper, N. C.; Edwards, P. P. Nuclear shielding in the alkali metal anions. *J. Am. Chem. Soc.* **1986**, *108*, 78-81.
- (15) Zurek, E. Alkali metals in ethylenediamine: A computational study of the optical absorption spectra and NMR parameters of  $[M(en)_3^{\delta+}\cdot M^{\delta-}]$  ion pairs. *J. Am. Chem. Soc.* **2011**, *133*, 4829-4839.
- (16) Abella, L.; Philips, A.; Autschbach, J. The sodium anion is strongly perturbed in the condensed phase even though it appears like a free ion in nuclear magnetic resonance experiments. *J. Phys. Chem. Lett.* **2020**, *11*, 843-850.
- (17) Szwarc, M. Ions and ion pairs. Acc. Chem. Res. 1969, 2, 87-86.
- (18) Bowron, D.T.; Soper, A. K.; Jones, K.; Ansell, S.; Birch, S.; Norris, J.; Perrott, L.; Riedel, D.; Rhodes, N. J.; Wakefield, S. R.; Botti, A.; Ricci, M.-A.; Grazzi, F.; Zoppi, M. NIMROD: The near and intermediate range order diffractometer of the ISIS second target station. *Rev. Sci. Instrum.s* **2010**, *81*, 033905.
- (19) Soper, A. K. GudrunN and GudrunX: Programs for Correcting Raw Neutron and X-ray Diffraction Data to Differential Scattering Cross Section, Rutherford Appleton Laboratory Technical Report No. RAL-TR-2011-013 (2011), also see https://epubs.stfc.ac.uk/.
- (20) Perdew, J. P.; Burke, K.; Ernzerhof, M. Generalized gradient approximation made simple. *Phys. Rev. Lett.* **1996**, *77*, 3865-3868. (21) Te Velde, G.; Bickelhaupt, F. M.; Baerends, E. J.; Fonseca Guerra, C.; van Gisbergen, S. J. A.; Snijders, J. G.; Ziegler, T. Chemistry with ADF. *J. Comp. Chem.* **2001**, *22*, 931-967.
- (22) Fonseca Guerra, C.; Snijders, J. G.; te Velde, G.; Baerends, E. J. Towards an order-N DFT method. *Theor. Chem. Acc.* **1998**, *99*, 391-403.
- (23) ADF, SCM, Theoretical Chemistry, Vrije Universiteit, Amsterdam, The Netherlands, http://www.scm.com.
- (24) Van Lenthe, E.; Baerends, E. J. Optimized Slater-type basis sets for the elements 1-118. *J. Comp. Chem.* **2003**, 24, 1142-1156.
- (25) Barrett, A. G. M.; Godfrey, Ch. R. A.; Hollinshead, D. M.; Prokopiou, P. A.; Barton, D. H. R.; Boar, R. B.; Joukhadar, L.; McGhie, J. F.; Misra, S. C. Dissolving metal reduction of esters to alkanes. A method for the deoxygenation of alcohols. *J. Chem. Soc.; Perkin Transactions I*, **1981**, 1501-1509.
- (26) Grobelny, Z.; Stolarzewicz, A.; Sokól, M.; Grobelny, J.; Janeczek, H. Enhanced stability of potassium solutions in tetrahydrofuran containing 15-crown-5. *J. Phys. Chem.* **1992**, *96*, 5193-5196.
- (27) Sakhanov, A. N. Investigations upon abnormal electrolytic dissociation. *J. Phys. Chem.* **1917**, *21*, 169-189.
- (28) Sakhanov, A. N.; Prscheborovsky, J. The conductivity and dissociation of silver nitrate in solvents with dielectric constant below 13. *J. Russ. Chem. Soc.* **1915**, *47*, 849-858.
- (29) Weingärtner. H. Corresponding states for electrolyte solutions. *Pure Appl. Chem.* **2001**, 73, 1733-1748.
- (30) Petrucci, S.; Eyring, E. M. Microwave dielectric relaxation, electrical conductance and ultrasonic relaxation of  $LiClO_4$  in polyethylene oxide dimethyl ether–500 (PEO-500). *Phys. Chem. Phys.* **2002**, *4*, 6043-6046.

- (31) Borodin, O.; Douglas, R.; Smith, G.; Eyring, E. M.; Petrucci, S. Microwave dielectric relaxation, electrical conductance, and ultrasonic relaxation of LiPF<sub>6</sub> in poly(ethylene oxide) dimethyl ether-500. *J. Phys. Chem. B* **2002**, *106*, 2140-2145.
- (32) Barthel, J.; Gerber, R.; Gores H. J. The temperature dependence of the properties of electrolyte solutions VI. Triple ion formation in solvents of low permittivity exemplified by  $\text{LiBF}_4$  solutions in dimethoxyethane. *Ber. Bunsenges. Phys. Chem.* **1984**, 88, 616-622.
- (33) Chen, Z.; Hojo, M. Relationship between triple ion formation constants and the salt concentration of the minimum in the conductometric curves in low-permittivity solvents. *J. Phys. Chem. B* 1997, 101, 10896-10902.
- (34) Bhattacharjee, A.; Roy, M. N. Ion association and solvation behavior of tetraalkylammonium iodides in binary mixtures of dichloromethane + N,N-dimethylformamide probed by a conductometric study. *Phys. Chem. Chem. Phys.* **2010**, *12*, 14534-14542.
- (35) Ekka, D.; Roy, M. N. Conductance, a contrivance to explore ion association and solvation behavior of an ionic liquid (tetrabutylphosphonium tetrafluoroborate) in acetonitrile, tetrahydrofuran, 1,3-dioxolane, and their binaries. *J. Phys. Chem. B* **2012**, *116*, 11687-11694.
- (36) Fleshman, A. M.; Petrowsky, M.; Frech, R. Application of the compensated Arrhenius formalism to self-diffusion: implications for ionic conductivity and dielectric relaxation. *J. Phys. Chem. B* **2013**, *117*, 5330-5337.
- (37) Cade, E. A.; Petenuci, J. 3<sup>rd</sup>, Hoffmann, M. M. Aggregation behavior of several ionic liquids in molecular solvents of low polarity-indication of a bimodal distribution. *Chem. Phys. Chem.* **2016**, *17*, 520-529.
- (38) Weingärtner, H.; Weiss, V. C.; Schröer, W. Ion association and electrical conductance minimum in Debye–Hückel-based theories of the hard sphere ionic fluid. *J. Chem. Phys.* **2000**, *11*3, 762-770.
- (39) Lee, B. S.; Lin, S. T. The origin of ion-pairing and redissociation of ionic liquid. *J. Phys. Chem. B* **2017**, *121*, 5818-5823.
- (40) Cavell, E. A. S.; Knight, P. C. Effect of concentration changes on permittivity of electrolyte solutions. *Z. Phys. Chem.* **1968**, 57, 331-4.
- (41) Petrucci, S.; Masiker, M. C.; Eyring, E. M. The possible presence of triple ions in electrolyte solutions of low dielectric permittivity. *J. Solution Chem.* **2008**, *37*, 1031–1035.
- (42) Levin, Y.; Fisher, M. E. Criticality in the hard-sphere ionic fluid. *Physica A: Statistical Mechanics and its Applications* **1996**, 225, 164-220.
- (43) Dyke, J.; Levason, W.; Light, M. E.; Pugh, D.; Reid, G.; Bhakhoa, H.; Ramasami, P.; Rhyman, L. Aza-macrocyclic complexes of the group 1 cations synthesis, structures and density functional theory study. *Dalton Trans.* **2015**, 44, 13853-13866.
- (44) Kuchenmeister, M. E.; Dye, J. L. Synthesis and structures of two thermally stable sodides with the macrocyclic complexant hexamethyl hexacyclen. *J. Am. Chem. Soc.* **1989**, *111*, 935-938.
- (45) Kuchenmeister, M. E. Synthesis and characterization of new alkalides and electrides via the tertiary amine complexing agents: Steps toward thermal stability (Doctoral thesis, Michigan State University, Michigan, 1989).
- (46) Millet, O.; Loria, J. P.; Kroenke, C. D.; Pons, M. & Palmer, A. G. The static magnetic field dependence of chemical exchange linebroadening defines the NMR chemical shift time scale. *J. Am. Chem. Soc.* **2000**, *122*, 2867–2877.
- (47) Martini, I. B.; Barthel, E. R.; Schwartz, B. J. Manipulating the production and recombination of electrons during electron transfer: Femtosecond control of the charge-transfer-to-solvent (CTTS) dynamics of the sodium anion. *J. Am. Chem. Soc.* 2002, 124, 7622-7634.

- (48) Bragg, A. E.; Cavanagh, M. C.; Schwartz, B. J. Linear response breakdown in solvation dynamics induced by atomic electron-transfer reactions. *Science* **2008**, 321, 1817-1822.
- (49) MacDonald, M. R.; Bates, J. E.; Ziller, J. W.; Furche, F.; Evans, W. J. Completing the series of +2 ions for the lanthanide elements: Synthesis of molecular complexes of Pr2+, Gd2+, Tb2+, and Lu2+. *J. Am. Chem. Soc.* **2013**, *13*5, 9857-9868.
- (50) http://hdl.handle.net/10477/79221.

# Table of Contents artwork:

